Nanotechnology **19** (2008) 405302 (5pp) doi:10.1088/0957-4484/19/40/405302

Growth of carbon nanofibers on nanoscale catalyst strips fabricated with a focused ion beam

Yusuke Ominami[1,3], Makoto Suzuki[2], Kiyotaka Asakura[1] and Cary Y Yang[2]

[1] Catalyst Research Center, Hokkaido University, Sapporo, Hokkaido 001-0023, Japan
[2] Center for Nanostructures, Santa Clara University, Santa Clara, CA 95053, USA

E-mail: yo136@pop.sys.hokudai.ac.jp

Received 15 May 2008, in final form 8 July 2008
Published 20 August 2008
Online at stacks.iop.org/Nano/19/405302

Abstract
We studied the growth mode of vertically aligned carbon nanofibers (CNFs) on Ni catalyst strips fabricated using a focused ion beam (FIB). We found that the CNF growth on Ni catalysts was strongly affected by the geometry of the microfabricated Ni catalyst strips. Selective growth of vertically aligned CNFs requires ion milling from the outside edge of the sample so that the milled materials are effectively evacuated. The CNF diameter and density on the strip depends on its width. Possible mechanisms to control CNF growth using microfabricated catalysts are analyzed with a liquid model using surface free energies.

1. Introduction

Vertically aligned nanowires such as carbon nanotubes (CNTs) and carbon nanofibers (CNFs) are promising for various applications ranging from sensors to interconnects [1–6]. Vertically aligned CNTs and CNFs grown on prefabricated microstructures are of particular interest. Recently, a focused ion beam (FIB) has been used to fabricate precisely controlled CNT microstructures such as atomic force microscopy (AFM) tips [7] and field emission (FE) tips [8]. The FIB is a powerful tool for making high-quality structures and devices in micro-electro-mechanical systems (MEMS) and integrated circuits [9, 10], because of its ability for direct fabrication of structures with feature sizes less than 100 nm.

Recently we reported a new preparation technique of CNFs on a fabricated microstructure using an FIB [11]. In this method, a narrow catalyst strip of 100 nm or less in width is fabricated for CNF growth. Subsequently, CNFs are selectively grown on the narrow strip using plasma-enhanced chemical vapor deposition (PECVD) [12]. We found that the growth mode of CNFs is controlled by the shapes and sizes of the microstructured strip which was covered with a Ni catalyst film. Upon heating, the size, shape, and location of the resulting catalyst particles are critical determining factors for the reaction to form CNFs. In general, fabricated catalysts are known to have unique catalytic properties [13–18]. Although the dependence of catalyst particles size and CNF diameter on the thickness of Ni catalyst thin film has been reported [19], it is not known how the geometry of the catalyst particle affects the growth of CNFs. In this paper, we report how the CNF growth is controlled by the size and the location of the catalyst strip fabricated using the FIB technique. We examine the relationship between the CNF size and the strip width and elucidate the mechanism of well-controlled CNF growth.

2. Experimental details

The samples were fabricated with an FIB system (HITACH FB-2100), in which a Ga^+ ion beam with an accelerating voltage of 40 keV with 40 nA is used. The dwell time was approximately 150 μs per pixel. The magnification is 4000. We adopted a slow single-pass ion beam. In our scan sequence, the final milling scan is performed toward the sidewalls of strip as shown by the arrows in figure 1. Thus materials sputtered by all scans except the final scan are never deposited on the sidewalls. Three areas with different geometries are milled. In the first area, two rectangle trenches are fabricated inside the sample, as shown in figure 1(a). The rectangular trench is milled toward the sidewall of the stripe. In the second area, while one rectangular trench is fabricated inside the sample like

[3] Author to whom any correspondence should be addressed.

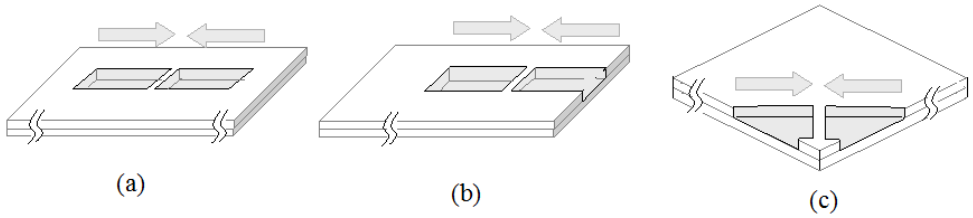

Figure 1. Schematic of samples with (a) two enclosed rectangle trenches. (b) Trenches milled from the inside and the edge of the sample. (c) Trenches milled toward the strip from both edges of the sample, all fabricated using FIB.

the first area, the other is milled from the edge of the sample, as shown in figure 1(b). In the third area, both rectangular trenches are fabricated toward the strip from the edges of the sample, as shown in figure 1(c). Each sample has a 30 nm Ti layer and a 35 nm Ni catalyst layer deposited using electron beam evaporation on a Si wafer. In order to characterize the relationship between the CNF size and the strip width, many narrow strips in the region from approximately 10 to 200 nm in width are prepared by controlling the milled position. CNFs are selectively grown on the narrow strip by PECVD. A gas mixture of NH_3:C_2H_2 (4:1) at a pressure of 4 Torr is used during the reaction process. The substrate temperature is estimated to be at least 600 °C. The details of CNF growth using PECVD have been reported previously [12]. The nanostructures of CNFs with various diameters and lengths on the strips have been characterized using scanning transmission electron microscopy (STEM) [20]. The CNFs have stacked graphitic layers and cup-shape structures. All narrow strips are imaged using scanning electron microscopy (SEM: Hitachi S-4800).

3. Results and discussions

3.1. Effect of location and geometry of microstructured catalysts

Figure 2 shows SEM images of the fabricated samples after CNF growth. Although vertically aligned CNFs grew on top of all strips, some of them reveal growth on the sidewalls depending on the growth conditions. Figure 2(a) shows the area where the strip lies between two enclosed rectangles in figure 1(a). There are bundles of carbon nanostructures with 5–10 nm diameter on both sidewalls. The growth occurred on the sidewalls because Ni catalysts were redeposited on both sidewalls during the FIB milling process. Figure 2(b) shows the area where strip borders the enclosed rectangular on one side and the open rectangle on the other, as indicated in figure 1(b). We could not find any carbon nanostructure growth on the open sidewall, while the other sidewall is covered by bundles of them, as observed in the first sample. This clearly shows that the Ni catalyst does not redeposit on the sidewall of the open rectangle. In the last picture, shown in figure 2(c), there is no carbon nanomaterial growth on both sidewalls which were fabricated from the edge of the sample and which are open, as indicated in figure 1(c). The results clearly show that the selective growth of CNFs on top of the strip requires ion milling from the outside edge of the sample

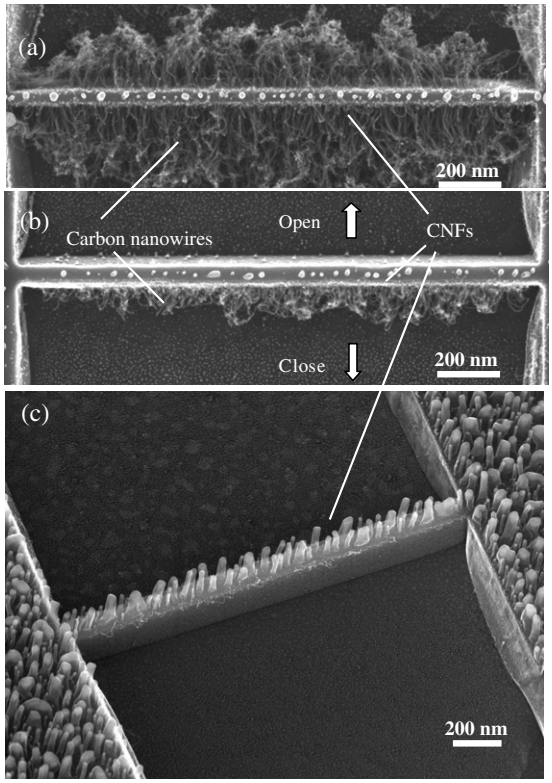

Figure 2. SEM images after CNF growth. (a) Area where the strip lies between two enclosed rectangular trenches shown in figure 1(a). (b) Area where the strip borders the enclosed rectangle on one side and the open rectangle on the other, as in figure 1(b). (c) Area fabricated from the edges of the sample and which is open, as in figure 1(c).

and open channels. This may be due to the fact that the milled Ni was effectively evacuated from the sample through the open channels while the milled Ni catalysts remain in the enclosed rectangle. Therefore, careful selection of geometry and location of the microstructured catalyst is needed to obtain well-controlled carbon nanostructures.

3.2. Effect of width of microstructured catalyst

Next we investigate the effect of the width of the strips on CNF growth. Figures 3(a) and (b) show the narrow strips with various widths before and after CNF growth. CNFs with approximately 10–100 nm diameter can grow on the strips. Figure 4 shows the minimum, average, and maximum

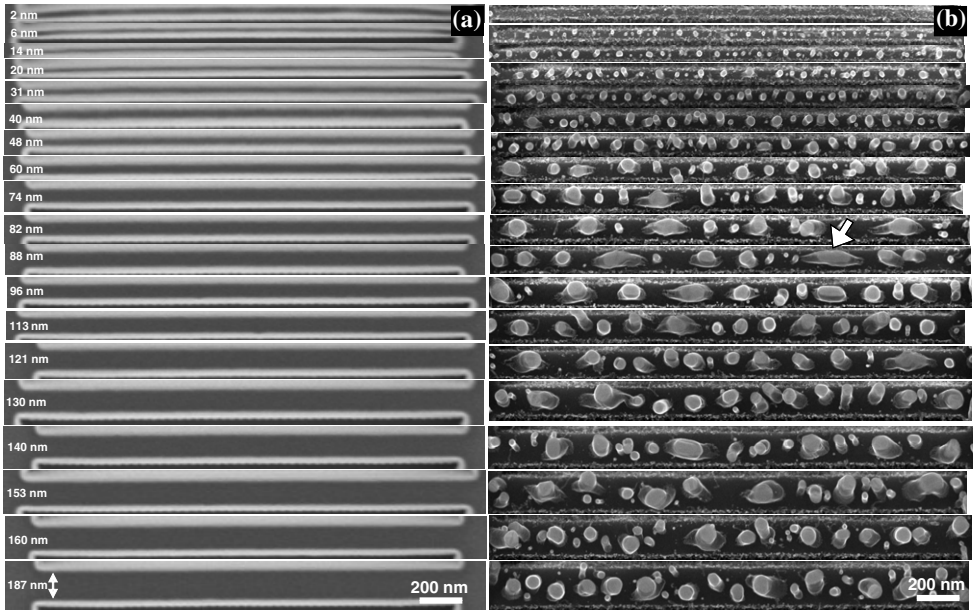

Figure 3. SEM images of the narrow strips (a) before and (b) after CNF growth with various widths.

diameters of CNFs on each narrow strip. The CNF diameter increases with the width of strip in the range from 10 nm to approximately 90 nm. Meanwhile, in the region of more than 90 nm, the minimum, average, and maximum diameters of the CNFs are constant irrespective of the width of the strip. The data clearly demonstrate that the CNF diameter can be controlled by the width of catalyst strip in the range of 90 nm or less. Figure 5 indicates the dependence of the number of CNFs per 1 μm strip length, as obtained from figure 3(b). We classify the effect of strip width into three regions. In region A (10 nm $<$ width $<$ 30 nm), the density of CNFs increases. In region B (30 nm $<$ width $<$ 90 nm), while the CNF diameter still increases with strip width, as shown in figure 4, the number of CNFs on the strips decreases. In region C (width $>$ 90 nm), where the average CNF diameter stays constant, the number of CNFs on the strip increases with increasing strip width.

In order to explain the strip-width-controlled CNF growth, we made following assumptions.

(i) The Ni particles are formed during the PECVD process and their sizes are mainly limited by the strip width.
(ii) The CNF diameter is almost the same as the Ni particle diameter, based on cross-sectional observation using TEM [11].
(iii) The CNFs grow only on Ni particles with their sizes greater than a certain critical size. Very small Ni particles may be poisoned by the surface carbon species.

In region A (figure 5), the Ni particle size is mainly regulated by the strip width. However, some Ni particles do not exceed the critical size for CNF formation. Consequently, they do not result in CNF growth, leading to an increase in density of Ni particles with larger than critical size with increase in catalyst strip width. Thus the density of CNFs increases with strip width. In region B, where all or most Ni particles on the strip can result in CNF growth, the CNF diameter increases

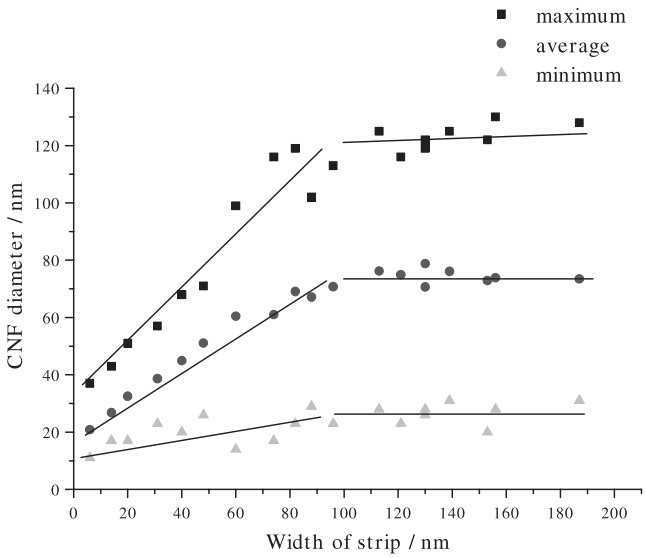

Figure 4. Plot of the minimum, average, and maximum diameters of CNFs on each strip width.

with strip width. However, the density of Ni particles decreases with increase in strip width because the Ni particles coalesce along the longitudinal direction, as indicated by the arrow in figure 3. In region C, the particle size of Ni is limited not by the strip width but by other factors discussed below. Consequently, the CNF diameter stops increasing.

The maximum Ni particle size is limited to approximately 90 nm, as shown in figures 2 and 3. This value can be explained based on the surface tensions of and interfacial tension between Ni and Ti layers under reaction conditions. Since the Ni catalyst film should be undergoing melting or premelting during substrate heating, judging from the particle shape which is hemispherical like a droplet, we can model the

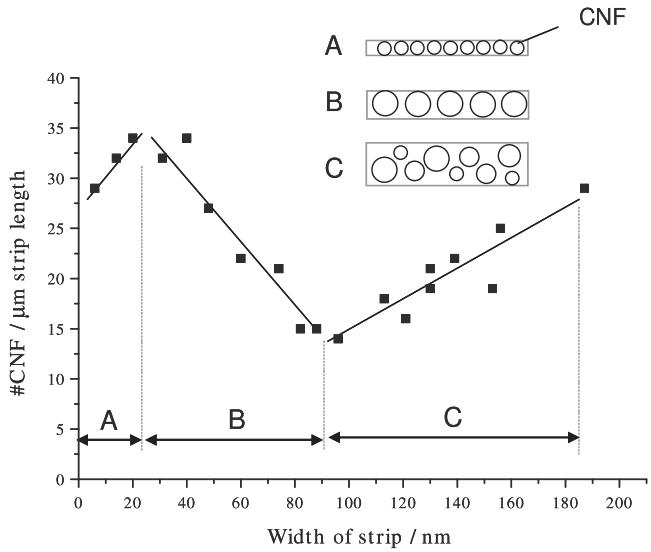

Figure 5. Dependence of the number of CNFs per 1 μm strip length on strip width.

particle as a hemisphere using

$$2h/\Delta = \tan\frac{\theta}{2}, \tag{1}$$

where h and Δ are the particle height and width, respectively, and Δ is a contact angle defined by

$$\gamma_{\mathrm{TiNi}} - \gamma_{\mathrm{Ti}} + \gamma_{\mathrm{Ni}}\cos\theta = 0. \tag{2}$$

A schematic diagram of the Ni particle model is shown in figure 6. Here γ_{Ni} and γ_{Ti} are the surface tensions of Ni and Ti, and γ_{TiNi} the interfacial tension between them. γ_{Ni} and γ_{Ti} are proportional to the bonding energies of Ni–Ni ($U_{\mathrm{Bond\_Ni}}$) and Ti–Ti ($U_{\mathrm{Bond\_Ti}}$), respectively, as follows [21].

$$\gamma_{\mathrm{M}} = U_{\mathrm{Bond\_M}}\frac{Z_{\mathrm{Ms}}}{Z_{\mathrm{M}}}\mathrm{N}_{\mathrm{Ms}} \tag{3}$$

where $Z_{\mathrm{Ms}}/Z_{\mathrm{M}}$ is the fractional number of bonds broken per surface atom M, and N_{Ms} is the areal density of surface atoms M. Ti and Ni have hcp and fcc crystal structures, with Ti–Ti and Ni–Ni radii 1.45 and 1.25 Å, respectively. Thus $\mathrm{N}_{\mathrm{Ms}}Z_{\mathrm{Ms}}/Z_{\mathrm{M}}$ for Ni and Ti are almost the same, and can be assumed to be equal. Also $\gamma_{\mathrm{Ti}}/\gamma_{\mathrm{Ni}}$ is approximately equal to $U_{\mathrm{Ni-Ni}}/U_{\mathrm{Ti-Ti}}$. The variation of interfacial tension between Ti and Ni (γ_{TiNi}) with the bond energy $U_{\mathrm{BOND\_TiNi}}$ can be obtained from equation (3), but it should be measured from the Ni and Ti atoms inside the Ni and Ti lattice. Thus γ_{TiNi} can be expressed as [22]

$$\gamma_{\mathrm{TiNi}} \cong U_{\mathrm{Bond\_TiNi}}\frac{Z_{\mathrm{TiNis}}}{Z_{\mathrm{TiNi}}}N_{\mathrm{TiNis}} - \frac{1}{2}\left(U_{\mathrm{Bond\_Ni}}\frac{Z_{\mathrm{Nis}}}{Z_{\mathrm{Ni}}}N_{\mathrm{Nis}} + U_{\mathrm{Bond\_Ti}}\frac{Z_{\mathrm{Tis}}}{Z_{\mathrm{Ti}}}N_{\mathrm{Tis}}\right). \tag{4}$$

If we use 200, 130, and 220 kJ mol^{-1} for $U_{\mathrm{Bond\_Ni}}$, $U_{\mathrm{Bond\_Ti}}$, and $U_{\mathrm{Bond\_TiNi}}$ predicted from [23] and all $\mathrm{N}_{\mathrm{Ms}}Z_{\mathrm{Ms}}/Z_{\mathrm{M}}$ are assumed to be equal, we calculate a contact angle of 70° from equations (2)–(4). Using this result and equation (1) for a Ni height of 35 nm, the particle width becomes 100 nm, in good agreement with the experimental results for CNF diameter given in figure 4. In this calculation, $\mathrm{N}_{\mathrm{Ms}}Z_{\mathrm{Ms}}/Z_{\mathrm{M}}$ for Ni and Ti were set to be equal. However, these values under most CNF growth conditions are not constant because the catalyst and underlayer consists of microcrystalline particles [20] in addition to the random Ni formation process. This probably causes the variation of CNF diameter as shown in figure 4. The thickness of Ni catalyst on the Si substrate for growth of CNFs approximately 100 nm in diameter is smaller [19], compared to the result in this paper. This is due to the fact that smaller surface free energy of Si than that of Ti makes γ in equations (1) and (2) larger. For better control of CNF growth on a narrow strip, the crystallographic condition of the metal underlayer or substrate should be investigated at the atomic and grain levels as well.

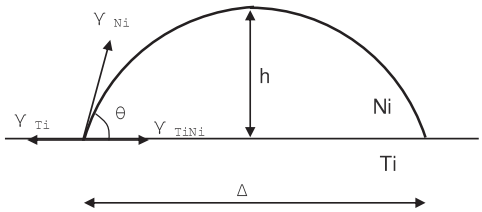

Figure 6. A schematic diagram of the Ni particle model on a Ti layer.

4. Concluding remarks

In this paper we present a study of the effect of geometry and location of catalysts, precisely created using the FIB technique, on the growth of carbon nanofibers. The scan sequence and geometry of the milled area critically affect the carbon nanomaterial growth on the sidewalls of the strips. The relationships of the measured CNF diameter and number density versus strip width have been examined in detail, and they correlate well. Further, using a hemispherical model for the catalyst particle, the predicted particle width of 100 nm is consistent with observation from SEM images and with results of CNF growth.

Acknowledgments

The authors are grateful to Drs Quoc Ngo, Alan M Cassell, and Jun Li of NASA Ames Research Center for helpful discussions and to Kevin Mcilwrath and Konrad Jarausch of Hitachi High-Technologies America for their expert assistance with FIB experiments.

References

[1] Javey A, Guo J, Paulsson M, Wang Q, Mann D, Lundstrom M and Dai H 2004 *Phys. Rev. Lett.* **92** 106804
[2] Guillorn A M, Melechko V A, Merkulov I V, Ellis D E, Britton L C, Simpson L M, Lowndes H D and Baylor R L 2001 *Appl. Phys. Lett.* **79** 3506

[3] Zhang L, Melechko V A, Merkulov I V, Guillorn A M, Simpson L M, Lowndes H D and Doktycz J M 2002 *Appl. Phys. Lett.* **81** 135
[4] Ngo Q, Cruden A B, Cassell M A, Sims G, Meyyappan M, Li J and Yang Y C 2004 *Nano Lett.* **4** 2403
[5] Li J, Stevens R, Delzeit L, Ng T H, Cassell A, Han J and Meyyappan M 2002 *Appl. Phys. Lett.* **81** 910
[6] Li J, Ye Q, Cassell A, Ng T H, Stevens R, Han J and Meyyappan M 2003 *Appl. Phys. Lett.* **82** 2491
[7] Deng Z, Yenilmez E, Reilein A, Leu J, Dai H and Molera A K 2006 *Appl. Phys. Lett.* **88** 23119
[8] Chai G and Chow L 2007 *Carbon* **45** 281
[9] Tseng A A 2004 *J. Micromech. Microeng.* **14** R15
[10] Gamo K 1993 *Semicond. Sci. Technol.* **8** 1118–23
[11] Ominami Y, Ngo Q, Kobayashi P N, Mcilwrath K, Jarausch K, Cassell M A, Li J and Yang Y C 2006 *Ultramicroscopy* **106** 597
[12] Cruden A B, Cassell M A, Ye Q and Meyyappan M 2003 *J. Appl. Phys.* **94** 4070
[13] Zuburtikudis I and Saltsburg H 1992 *Science* **258** 1337
[14] Graham D M, Kevrekidis G Y, Asakura K, Lauterbach J, Rotermund H H and Ertl G 1994 *Science* **264** 80–2
[15] Asakura K, Lauterbach J, Rotermund H H and Ertl G 1994 *Phys. Rev.* B **50** 8043–6
[16] Ohminami Y, Suzuki S, Matsudaira N, Nomura T, Chun J W, Ijima K, Nakamura K, Mukasa K, Nagase M and Asakura K 2005 *Bull. Chem. Soc. Japan.* **78** 435–42
[17] Laurin M, Johanek V, Grant W A, Kasemo B, Libuda J and Freund J H 2005 *J. Chem. Phys.* **122** 084713
[18] Rioux M R, Song H, Grass M, Habas S, Niesz K, Hoefelmeyer D J, Yang P and Somorjai A G 2006 *Top. Catal.* **39** 167–74
[19] Chhowalla M, Teo B K, Ducati C, Rupesinghe L N, Amaratunga A G, Ferrari C A, Roy D, Robertson J and Milne I W 2001 *J. Appl. Phys.* **90** 5308
[20] Ominami Y, Ngo Q, Suzuki M, Austin J A, Cassell M A, Li J and Yang Y C 2006 *Appl. Phys. Lett.* **89** 263114
[21] Zangwill A 1988 *Physics at Surface* (New York: Cambridge University Press)
[22] Becker R 1938 *Ann. Phys.* **32** 128
[23] Luo Y 2007 *Comprehensive Handbook of Chemical Bond Energies* (Boca Raton, FL: CRC press)